Food Hydrocolloids 99 (2020) 105317

Contents lists available at ScienceDirect

Food Hydrocolloids

journal homepage: www.elsevier.com/locate/foodhyd

Effects of sucrose addition on the rheology and structure of iota-carrageenan

Dongying Yang[a,b], Shuai Gao[a], Hongshun Yang[a,b,*]

[a] Department of Food Science & Technology, National University of Singapore, Singapore 117543, Singapore
[b] National University of Singapore (Suzhou) Research Institute, 377 Lin Quan Street, Suzhou Industrial Park, Suzhou, Jiangsu, 215123, PR China

ARTICLE INFO

Keywords:
Iota carrageenan
Sucrose
Rheology
Gelation
Mechanism
Stabili
s
ation effect

ABSTRACT

Sucrose addition contributes to the rheology of carrageenan, which improves the quality of food that includes carrageenan as an additive. In the present study, the rheological behaviours of sucrose-supplemented iota carrageenan at different concentrations (0–20%, w/v) were determined. Easier gelation with a higher gelling temperature (51.4–57.4 °C) could be achieved by sucrose addition, and the trend could be predicted using mathematical models. Application of the Kirkwood-Buff theory demonstrated that exclusion effects of water and direct binding between sucrose and iota carrageenan are the possible mechanisms for the stabilisation, which act by providing significantly greater $|\Delta G_{u2}|$ than $|\Delta G_{u1}|$ from all samples using Clausius-Clapeyron equation ($|\Delta G_{u1}|$ and $|\Delta G_{u2}|$ are calculated KB parameters representing the contribution of the rearrangement of water and co-solvent around the solute to the thermodynamics of sol-gel transition). Fourier transform infrared spectroscopy further confirmed the bindings by detecting band shifts (from 845 to 835 cm^{-1}). The gel was the strongest (251.71 Pa) at 5% (w/v) sucrose; however, too much sucrose decreased the gel strength. The Winter-Chambon equation provided the fractal dimension d_f (2.22) and critical gel strength $S_{g\ (12.52\ Pa \bullet s^n}$ at 5% (w/v) sucrose concentration, indicating the highest density and critical strength. The zeta potential (−0.92 mV) and confocal laser scanning microscopy images also showed the most abundant aggregates at 5% sucrose. Excess sucrose may form sucrose-sucrose hydrogen bonds that loosen the iota carrageenan network. A schematic representation was provided to show how sucrose could affect the structure and gelation of iota carrageenan (differs from kappa carrageenan) and the potential bonds related to the effect.

1. Introduction

Carrageenan comprises a group of linear sulphated galactans obtained from red seaweed, among which, kappa-carrageenan (KC) and iota-carrageenan (IC) are used ubiquitously in the food industry for their thickening and gelling abilities (Huang & Yang, 2019; Lennart; Parker, Brigand, Miniou, Trespoey, & Vallée, 1993; Piculell, Nilsson, & Muhrbeck, 1992). KC and IC share a similar disaccharide backbone of alternating 3-linked β-D-galactopyranose (G) and 4-linked α-D-galactopyranose (D), as well as the cyclisation form of D units (DA). The sulphation status (S), including the position and amount, classify different carrageenan types (Bixler & Porse, 2011). Therefore, KC (G4S-DA) and IC (G4S-DA2S) differ from each other in terms of their molecular structures. As a result, their rheological properties and behaviours in food products also vary. IC tends to produce more elastic gels with lower hysteresis compared with those comprising KC (Zia et al., 2017). By applying IC to food systems, the spectrum of carrageenan usage has increase to fulfil the diversity required by food products.

Apart from its intrinsic structural variation, there is also a series of parameters that determine the properties of IC, such as combinations with other polysaccharides, proteins, cations, and small molecules, resulting in novel rheological properties of carrageenan (Agoda-Tandjawa, Le Garnec, Boulenguer, Gilles, & Langendorff, 2017; Nguyen, Nicolai, Benyahia, & Chassenieux, 2014; Yang, Yang, & Yang, 2018b). Recent studies are more interested in the cosolvents which have electrostatic interactions with carrageenan such as amino acids and proteins (Dong et al., 2019; Li et al., 2019). However, sucrose, a commonly used sweetener in real food systems, not only adds sweetness but also influences the texture. The sweetness and texture properties may interact and generally, for IC-containing desserts, sucrose enhances springiness and firmness (Lethuaut, Brossard, Rousseau, Bousseau, & Genot, 2003). For the mechanism of the effect of sucrose on the rheology and structure of KC, several hypotheses have been put forward. Exclusion effects of water and binding between sucrose and gel-state KC are thought to be most plausible explanations for the observed behaviour (Stenner, Matubayasi, & Shimizu, 2016). However, for IC, the effect of sucrose requires further investigation.

Rheological tests offer explicit analysis of the viscoelastic

* Corresponding author. Food Science and Technology Programme, c/o Department of Chemistry, National University of Singapore, 117543, Singapore.
E-mail address: chmynghs@nus.edu.sg (H. Yang).

https://doi.org/10.1016/j.foodhyd.2019.105317
Received 27 April 2019; Received in revised form 31 July 2019; Accepted 19 August 2019
Available online 22 August 2019
0268-005X/

properties, guiding the design and performance of food during consumption, such as mastication and digestion (Pang et al., 2019; Soukoulis, Fisk, Gan, & Hoffmann, 2016; Yang et al., 2015). Based on rheological tests, various mathematical models have been introduced to better understand and describe the structure and property of gelling systems, including the power law model (analysing frequency sweep results to better understand the viscoelasticity) (Diañez et al., 2019), the Winter-Chambon model (based on frequency sweeps close to gelling points, giving critical gelling temperature and the density of the structures) (Rafe & Razavi, 2017), and the Kirkwood-Buff (KB) theory (using melting temperature changes to further investigate the thermodynamic properties and the contribution of sucrose to IC gelation) (Kirkwood & Buff, 1951). Combining experimental and model fitting results could reveal the effect of sucrose on IC gelation.

The objectives of the present study were to investigate and interpret the effect of different concentrations of added sucrose on the rheology of IC solutions. Analytical methods including Fourier transform infrared (FTIR) spectroscopy and confocal laser scanning microscopy (CLSM) were applied. The results suggested the potential mechanisms of the effect of sucrose on IC gelation.

2. Materials and methods

2.1. Materials and sample preparation

Analytical grade (AR) chemicals and standards, including sucrose and the dye fluorescein isothiocyanate (FITC), were obtained from Sigma Aldrich (St. Louis, MO, USA). Commercial grade iota carrageenan (IC) was also obtained from Sigma Aldrich as CARRAGEENAN TYPE II. Potassium bromide (KBr) and dimethyl sulphoxide (DMSO) were bought from Merck KGaA (Darmstadt, Germany).

Deionised water (DI water) was prepared using a Milli-Q purification system (Millipore, Billerica, MA, USA). Sunflower oil used as cover oil in the rheological tests was bought from a local supermarket in Singapore. IC at 2% (w/v) was prepared for the rheological test and sucrose was dry mixed with IC at concentrations of 0, 2.5, 5, 10, and 20% (w/v).

2.2. Zeta potential

The samples above were diluted to 40 × with hot water and subject to zeta potential measurements using a Zeta Potential analyser (Brookhaven Instruments, Holtsville, NY, USA) with dynamic light scattering (DLS). The angle of DLS was set at 173° and Smoluchowski's model was applied (Sow, Kong, & Yang, 2018).

2.3. Rheological tests

A rotational Anton Paar MCR 102 stress-controlled rheometer (Anton Paar, Graz, Austria) with stress control was used to perform the rheological measurements. A stainless-steel parallel plate (diameter: 25 mm and gap: 1 mm) was chosen to test the IC samples. The samples were stirred at 90 °C for 60 min to achieve complete dispersion of the solutes. Then, approximately 1 mL of hot sample was transferred onto the preheated plate and the redundant sample was trimmed off before starting the test. Sunflower oil was used to cover the edge of sample to prevent water evaporation during measurement. The following sweeps were then conducted while recording the storage modulus (G') and loss modulus (G') (Ali, Kishimura, & Benjakul, 2018): (a) Cooling (from 90 °C to 10 °C) and melting (from 10 °C to 90 °C) were measured at the rate of 1 °C/min with an angular frequency of 1 1/s and a strain of 1%; (b) A constant temperature sweep (10 °C) after cooling for 180 min under the same conditions as (a) to stabilise the gel; (c) A frequency sweep (10–0.1 1/s) was conducted at the gel state (10 °C) with a constant strain of 1% (Motta Romero, Santra, Rose, & Zhang, 2017). The power law was used to fit the frequency sweep result:

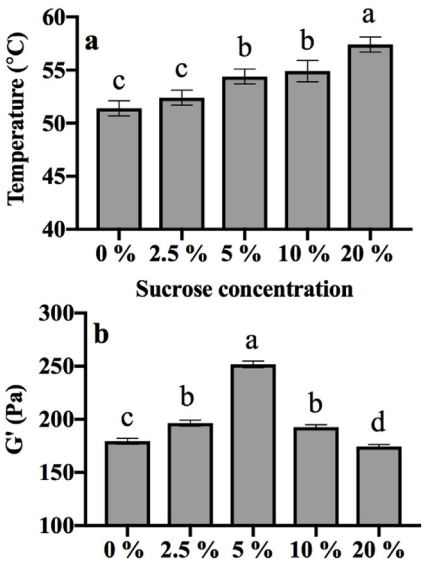

Fig. 1. (a) Gelling temperature and (b) gel strength (storage modulus G′ at 25 °C) of 2% (w/v) iota carrageenan (IC) with 0%, 2.5, 5, 10, and 20% (w/v) sucrose. *Within each parameter, means and standard derivations with different lowercase letters were significantly different ($P < 0.05$) among different groups.

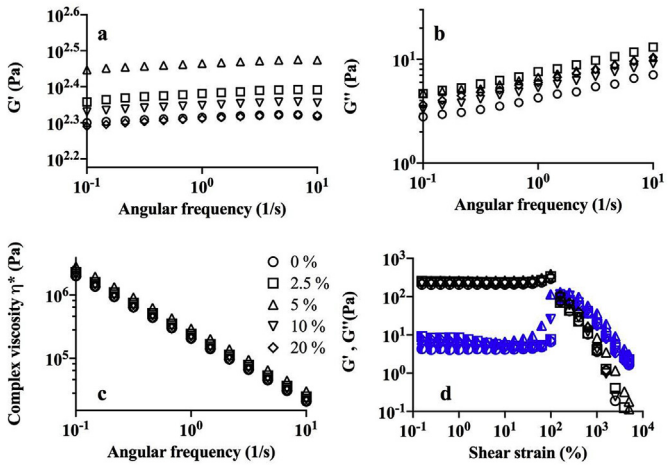

Fig. 2. (a) Storage modulus G′, (b) loss modulus G″ and (c) complex viscosity η* under a frequency sweep, (d) storage modulus G' (empty symbols) and loss modulus G" (half solid symbols) under a strain sweep of 2% iota carrageenan (IC) (w/v) with 0, 2.5, 5, 10, and 20% (w/v) sucrose.

$$G' = A\omega^n \tag{1}$$

where ω stands for the angular frequency (1/s), A is the gel strength, and n is the relaxation exponent indicating the correlation in the gel network. (Gabriele, de Cindio, & D'Antona, 2001);

(d) A strain sweep (0.1–1000%) was also performed at the gel state from (b), with a fixed frequency of 1 1/s. Deformation occurred during strain sweep; therefore, the critical strain, which signifies the start of structure breakdown, could be obtained. Using the critical strain and the corresponding storage modulus, the cohesive energy (E_c) could be calculated using Equation (2).

$$E_C = \int_0^{\gamma_{cr}} G'\gamma_{cr}\delta\gamma = \frac{1}{2}\gamma_{cr}{}^2 G' \tag{2}$$

where γ_{cr} is the critical strain (cr, critical) and G′ is the storage modulus.

(e) A frequency sweep at temperatures around the gelling points was conducted under the same conditions in (c) to illustrate the critical gelling points according to the Winter-Chambon equation, based on the

Table 1
Power Law model fitting, cohesive energy density (E_c) calculation, and Kirkwood-Buff theory calculation of 2% iota carrageenan (IC) (w/v) with 0%, 2.5%, 5%, 10% and 20% (w/v) sucrose.

Composition		0%	2.5%	5%	10%	20%
Power Law	A (10^3 Pa*s$^{(1-n)}$)	2.06 ± 0.01^d	2.40 ± 0.01^b	2.91 ± 0.01^a	2.22 ± 0.01^c	2.04 ± 0.01^e
	n (10^{-2})	98.9 ± 0.1^a	98.3 ± 0.1^c	98.6 ± 0.1^b	98.7 ± 0.1^b	98.4 ± 0.2^c
Cohesive energy density (E_c) (J/m^3)		99.42 ± 5.89^b	103.46 ± 19.57^b	163.26 ± 8.99^a	133.67 ± 12.32^{ab}	124.02 ± 14.61^b
Kirkwood-Buff theory	Melting temperature (T_m) (°C)	52.75 ± 0.58^d	54.08 ± 0^c	55.75 ± 0.58^b	56.08 ± 0.01^b	58.75 ± 0.58^a
	$\Delta T_m/\Delta C$ (K/mol/L)	–	18.21	20.54	11.40	10.27
	ΔS (cal/K mol of cross-link junctions)	−47.2	−47.2	−47.2	−47.2	−47.2
	Water activity	1	0.999	0.998	0.996	0.992
	ΔV_u (cm^3 g^{-1})	8.5	8.5	8.5	8.5	8.5
	-ΔG_{u1} (cm^3 mol^{-1})	–	−8.86	−8.91	−8.50	−8.70
	-ΔG_{u2} (cm^3 mol^{-1})	–	−464.35	−522.37	−293.41	−264.66

Note that mol^{-1} here refers to per mol of intermolecular cross-links and the value of ΔS (cal/K mol of cross-link junctions) and ΔV_u (cm^3 g^{-1}) are taken from Gekko (Gekko & Kasuya, 1985; Gekko et al., 1987). *Within each row, means with different lowercase letters are significantly different ($P < 0.05$) among different groups.

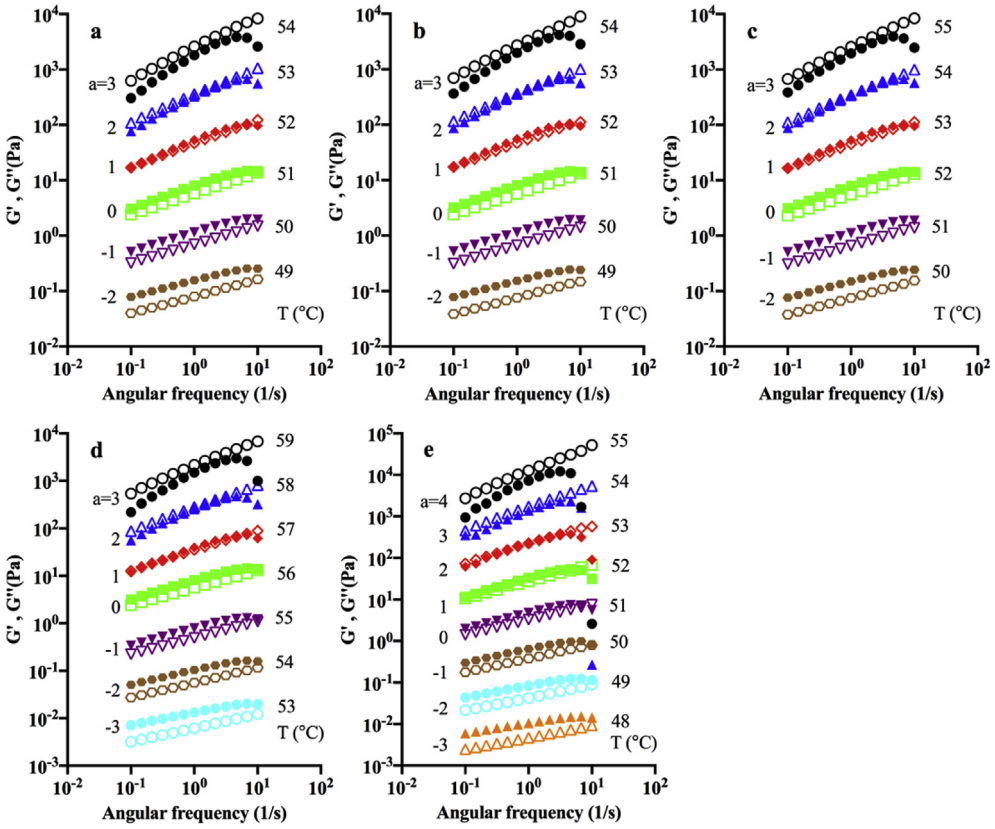

Fig. 3. Dependence of storage modulus G' (solid symbol) and loss modulus G" (open symbol) as a function of angular frequency (1/s) for 2% iota carrageenan (IC) (w/v) solutions with the addition of sucrose (a) 0%, (b) 2.5%, (c) 5%, (d) 10%, and (e) 20% (w/v).

power law relationship between G', G' and frequency (ω):

$$G'(\omega) \sim G'(\omega) \sim \omega^n \tag{3}$$

where n is the dynamic power law exponent within the range of 0–1, in which n = 1 represents the elastic state and n = 0 indicates the viscous state (Liu & Li, 2016).

The value of n from equation (4) can be used to calculate the fractal dimension (d_f), which represents the density of the structure, according to equation (4).

$$n = \frac{d(d+2-2d_f)}{2(d+2-d_f)} \tag{4}$$

where d = 3 for the space dimension.

In addition, the shear relaxation modulus G(t) can be represented using equation (5):

$$G(t) = S_g t^{-n} \tag{5}$$

where S_g is the critical gel strength. To calculate S_g, equation (6) can be applied using G', G' and critical gelling point.

$$G'(\omega) = G''(\omega)/\tan\left(\frac{n\pi}{2}\right) = S_g \omega^n \Gamma(1-n)\cos\left(\frac{n\pi}{2}\right) \tag{6}$$

where $\Gamma(1-n)$ is the Gamma function (Rafe & Razavi, 2017).

2.4. KB theory

The KB theory has been used to investigate mechanisms related to the impact of sucrose on the gelation of hydrocolloids such as gelatin, KC, and agarose (Shimizu & Boon, 2004; Shimizu, Stenner, & Matubayasi, 2017; Stenner et al., 2016). Using the combination of KB theory and Clausius-Clapeyron equation, KB parameters like ΔG_{u1} and

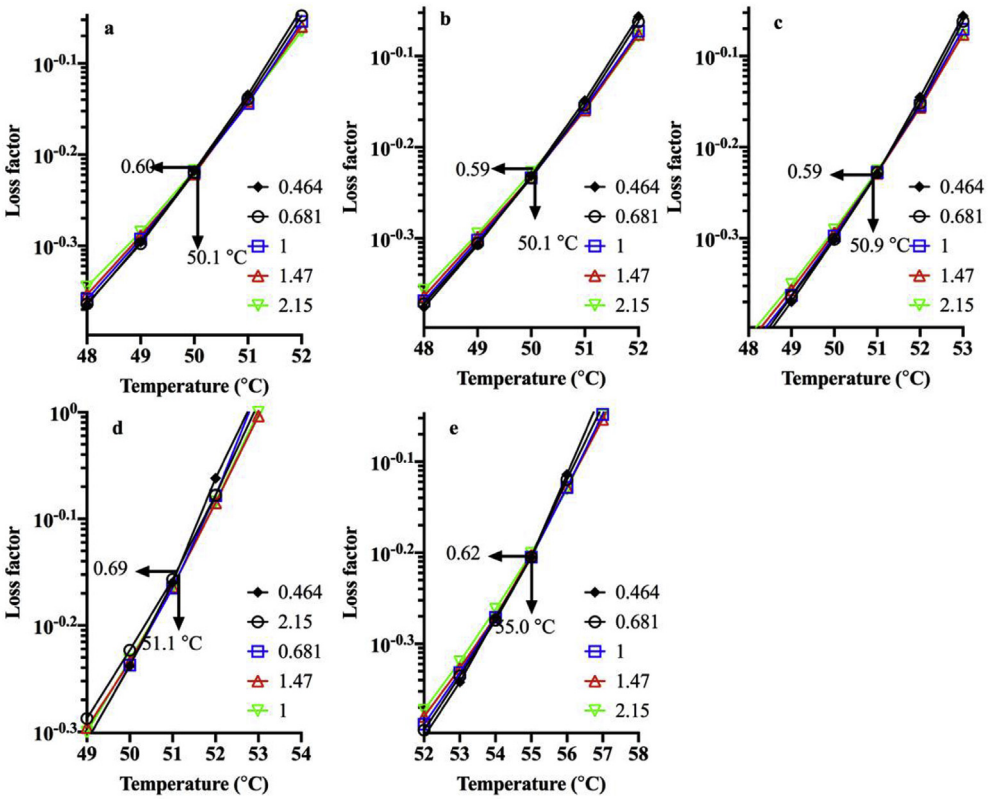

Fig. 4. Dependence of the loss factor as a function of temperature (°C) with different angular frequencies (1/s) for 2% iota carrageenan (IC) solutions with the addition of sucrose at (a) 0%, (b) 2.5%, (c) 5%, (d) 10%, and (e) 20% (w/v).

ΔG_{u2} (representing the contribution of the rearrangement of water and cosolvent around the solute to the thermodynamics of sol-gel transition) could be calculated to describe the mechanism.

$$\Delta G_{u1} = -\frac{n_2 V_2}{n_1}\Delta S_{g\to s}\frac{\delta T_{g\to s}}{\delta \mu_1} - \Delta V_u \tag{7}$$

$$\Delta G_{u2} = V_1 \Delta S_{g\to s}\frac{\delta T_{g\to s}}{\delta \mu_1} - \Delta V_u \tag{8}$$

$$n_1 V_1 + n_2 V_2 = 1 \tag{9}$$

In Eqs. (7) and (8), $\Delta S_{g\to s}$ is the entropy change during melting; $\delta T_{g\to s}$ represents the change of melting temperature; ΔV_u represents the volume change during melting; n_1 and n_2 are the bulky concentration of water (55.6 mol/L) and sucrose, respectively; $\delta \mu_1$ is the change of chemical potential of water and the value can be calculated using $RT \ln \alpha$ where α is the water activity; and R is the gas constant. Among these, $\Delta V_{g\to s}$ and $\Delta S_{g\to s}$ were taken from the reports from Gekko's group (Gekko & Kasuya, 1985; Gekko, Mugishima, & Koga, 1987), while the dependence of gelling temperature on the water chemical potential was inferred from the rheological tests performed in the present study. Eq. (9) can also be used for the calculation based on the approximation in KB theory: the concentration of carrageenan $u \to 0$. For consistency, the calculation was based on per mole of crosslinks. ΔG_{u1} expresses the thermodynamic contribution from water structure change and ΔG_{u2} summarises the thermodynamic contribution from cosolvents like sucrose. During melting, both ΔG_{u1} and ΔG_{u2} are negative since the melting sacrifices the density as well as the attractive interaction. Therefore, the absolute values of $\Delta G_{u1}$and ΔG_{u2} can be used to compare the contributions and find out the driving forces responsible for the effect of sucrose on carrageenan gelation.

2.5. FTIR

The gels set according to methods in section 2.3 were freeze-dried to conduct solid phase analysis. The freeze-dried samples were homogenised with pre-dried KBr to produce a KBr pellet. Before sample scanning, air scanning was conducted as a background spectrum at room temperature within the wave number range of 4000–500 cm^{-1} on a PerkinElmer Spectrum One FTIR spectrometer (PerkinElmer, Waltham, MA, USA). Sample scanning was then performed using the same method. Transmission of the samples was recorded and processed using Spectrum software version 6.3.2 (Sow, Tan, & Yang, 2019).

2.6. CLSM

The IC in the various samples was stained before testing using FITC (excitation and emission wavelengths of 495 and 525 nm, respectively) according to previous reports (Sow, Chong, Liao, & Yang, 2018; Sow, Toh, Wong, & Yang, 2019). FITC was dissolved in DMSO (2%, w/v) as a stock dye solution. The pH of the sample solution (2%, w/v) was pre-adjusted to 8.5 to induce dye binding. Then, 25 μL of dye solution was added into 100 mL of the sample and maintained at room temperature for 90 min. Before testing, the pH of the mixture was re-adjusted to the original value. The samples were imaged at the solution state (0.5%, w/v) and the gel state (2%, w/v). The solution sample (20 μL) was dripped onto a cover glass slide (0.13–0.16 mm thickness) while the gel sample (20 μL) was added into a glass well. The samples were stored overnight at 4 ± 2 °C in the dark. An Olympus Fluoview FV 3000 confocal scanning unit (Tokyo, Japan) equipped with argon ion and Helium–Neon (HeNe) lasers was used to examine the microstructures. Images were taken under water immersion at 60× magnification (PlanApo 60 × /1.0 WLSM 0.17). ImageJ software (National Institutes of Health, Bethesda, Maryland, USA) was used to process the acquired images.

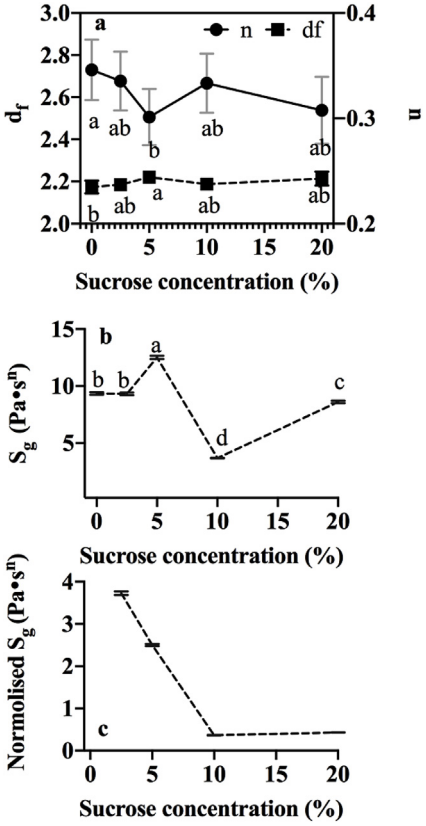

Fig. 5. Dependence of (a) the critical relaxation exponent n and fractal dimension d_f, (b) the critical gel strength S_g and (c) the normalised critical gel strength for 2% iota carrageenan (IC) (w/v) solutions with the addition of sucrose at (a) 0%, (b) 2.5%, (c) 5%, (d) 10%, and (e) 20% (w/v).

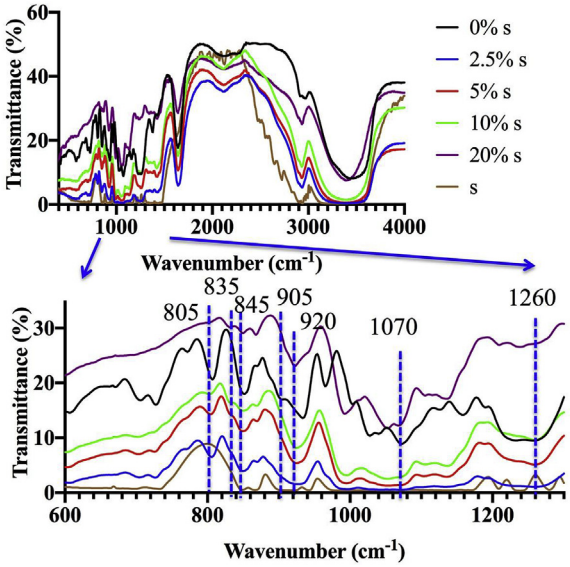

Fig. 6. Fourier transform infrared (FTIR) spectra of iota carrageenan (IC) with addition of 0, 2.5, 5, 10, and 20% (w/v) sucrose. Pure sucrose was also included as a reference.

2.7. Statistical analysis

Each test was repeated at least three times independently. The results are expressed as the mean ± the standard deviation (SD). Statistical differences within and between test groups were determined using one-way ANOVA ($P < 0.05$) and Student's t-test in the JMP software (SAS, Cary, NC, USA).

3. Results and discussion

3.1. Effect of sucrose addition on gelling behaviours of IC

Fig. 1 shows that the gelling behaviours varied according to the concentration of added sucrose within the range of 0–20%. For the gelling temperature as shown in Fig. 1a, there was an obvious increasing trend indicating easier gel formation induced by sucrose. This result was similar to that found for KC: co-solvents like sucrose shift the equilibrium of sol-gel transition towards gel formation (Sharma Khanal et al., 2019; Stenner et al., 2016). Therefore, within this range, adding sucrose allows adjustment of the gelling point of IC, providing more flexibility for food design. Moreover, linear model could describe the relationship between the sucrose concentration and gelling points as $y = 1.5025x + 49.696$ ($R^2 = 0.987$). Accordingly, predictable gelling points could be achieved.

However, the trend of gel strength for IC with added sucrose seemed not to agree with that of KC, for which gel strength is enhanced by sucrose addition (Gekko et al., 1987). As shown in Fig. 1b, the gel strength of the IC solution increased at sucrose concentrations up to 5%, after which the gel strength decreased, suggesting that higher sucrose levels reduce the strength of the structure produced by IC. Although facilitated by sucrose, IC appears to possess lower critical concentration (5% w/v) in terms of gel strength comparing with that of KC (45 wt%). This can be explained in terms of the gelling mechanism differences between KC and IC: Comparing to KC, IC relies less on helix aggregation, leading to less hysteresis and more elasticity in IC gels (Brenner, Tuvikene, Parker, Matsukawa, & Nishinari, 2014; Piculell, 2006). Moreover, sucrose has been reported to facilitate the aggregation of KC (Watase, Nishinari, Williams, & Phillips, 1990). IC, with solely aggregation, may have fewer sites for sucrose to function.

Frequency sweeps of gels, as shown in Fig. 2a and b, showed an increase in both modulus values, with more frequency-dependent G' than G', confirming a more solid-like rheological behaviour (Zhong & Ikeda, 2012). Fig. 2c displays the dependence of complex viscosity on frequency, as well as the mechanical strength of the gels. The linear decrease suggests the shear thinning property of all gels. In addition, the viscosity relates to mouth feel (Piorkowski & McClements, 2014). In other words, not only the preparation and storage, but also the texture of food products is associated with sucrose concentration. Thus, sucrose addition at 5% achieved the best thickening effect among the concentrations used.

Power law model fitting results ($R^2 > 0.99$ for all samples) are listed in Table 1. The pre-exponential factor A indicates the gel strength of the structure and consistently, 5% sucrose concentration provided the strongest gel. The relaxation exponent n is positively associated with the rigidity of the structure since increasing n indicates more entangled and associated systems (Wu et al., 2018). Therefore, when $n = 1$, the sample is completely elastic. Sucrose addition seemed to reduce the rigidity and elasticity while generating a more flexible structure.

Strain sweep was also tested to illustrate the large deformation properties of the samples, and the recorded G′ according to strain is shown in Fig. 2d. All the samples seem to behave similarly, with almost strain-independent G′ and G″ values, which allows the determination of linear viscoelastic region (LVR). Meanwhile, G′ was significantly greater than G″, demonstrating that the gel state was present since G′ measures the stored energy and the elastic portion while G″ measures the energy dissipated as heat and the viscous portion. When G' > 10G″, it is treated as a typical gel (Zhou & Yang, 2019). Then, as the strain increases, the gels start to break, causing uneven reductions of both G′ and G". The cross-point marks the critical strain. From the strain sweep results, sucrose addition seems not to affect the critical strain of IC. Knowing the critical strain allowed us to calculate the cohesive energy

Table 2
FTIR peaks location and assignment of 2% iota carrageenan (IC) (w/v) with 0%, 2.5%, 5%, 10% and 20% (w/v) sucrose.

Peak wavenumber (cm^{-1})						Assignments
0%	2.5%	5%	10%	20%	sucrose	
1260	1260	1260	1260	–	–	O = S=O of sulphated esters
–	–	–	–	943	943	C–H deformation vibration (sucrose)
905	920	920	920	920	–	C–O–SO_4 on C_2 of 3,6-anhydrogalactose (DA2S)
845	835, 845	835, 845	835, 845	835, 845	–	C–O–SO_4 on C_4 of galactose-4- sulphate (G4S)
805	805	805	805	805	–	C–O–SO_4 on C_2 of 3,6-anhydrogalactose (DA2S)

Note that the assignments are taken from previous reports (Pereira et al., 2009; Yang et al., 2018a, b).

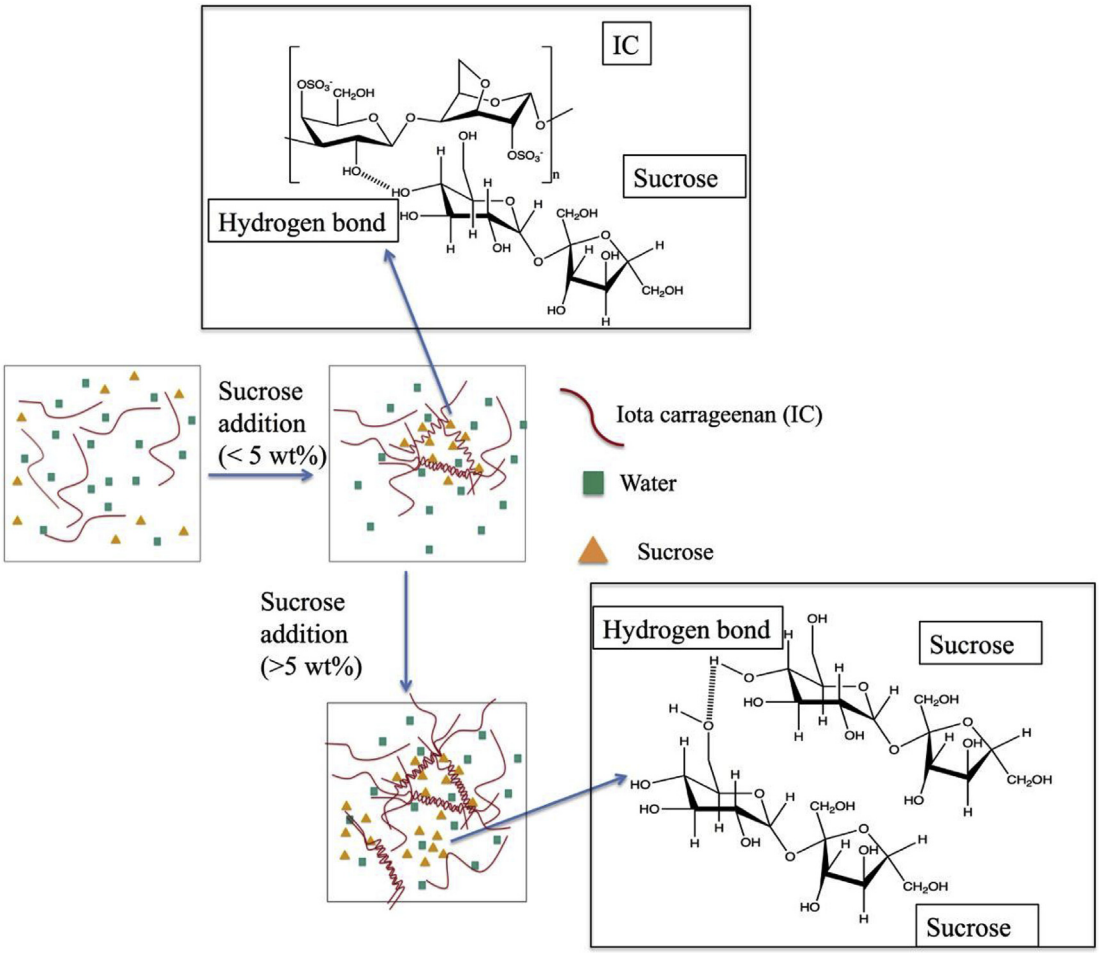

Fig. 7. Schematic presentation of the enhancement effect produced by sucrose on iota carrageenan (IC) gelation: a lower amount of added sucrose (< 5%, w/v) supported the formation of hydrogen bonds between IC and sucrose and increased the gel strength by increasing the density of the network; a higher amount of added sucrose (> 5%, w/v) also stabilised the gel but increased the opportunity for sucrose-sucrose hydrogen bonds to loosen the network, causing a reduction in gel strength.

density (E_c) (Table 1), further expressing the strength of the structure. The results also showed that 5% sucrose addition results in greater gel strength.

3.2. Effect of sucrose addition on critical gelling properties according to the Winter-Chambon equation

Frequency sweep at temperatures close to the gelling temperature of IC with different amount of sucrose are shown in Fig. 3. To reduce overlapping, the data have been shifted vertically by a factor of 10^a. A similar pattern was found among all concentrations of sucrose addition: at temperatures above the gelation point, G″ outnumbered G′ during the frequency sweep; as the temperature approached the gelling temperature, G′ increased while G″ decreased, converging towards the same value. After the gel set, G′ was always larger than G″ and they shared a similar dependence on frequency. In the intermediate state before gel setting, a plateau was detected in the G′ curve that could be related to the entanglement of polymer branches (Covis et al., 2016).

The critical gelling temperature, regardless of the frequency, can be obtained using a frequency sweep close to the gelling points, as shown in Fig. 4. At the gelling point, loss factor, which can be calculated with G'/G″, therefore equals to 1. The gelling temperatures obtained from different frequencies intersect with each other, providing the critical gelling point, which indicates independence of frequency (Yang, Yang, & Yang, 2018a). An increasing trend (50–55 (°C)) was found for the critical gelling points according to Fig. 4. Increased gel-formation

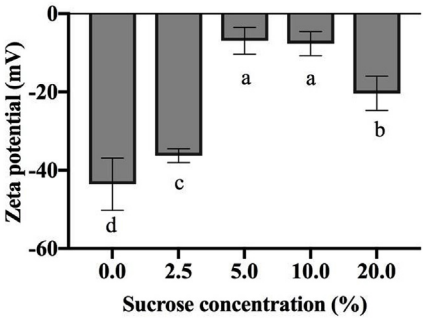

Fig. 8. Zeta potential of 2% iota carrageenan (IC) (w/v) with 0, 2.5, 5, 10, and 20% (w/v) sucrose (diluted to 0.5% IC w/v). *Within each parameter, means and standard derivations with different lowercase letters are significantly different ($P < 0.05$) among different groups.

induced by sucrose addition was further confirmed. However, unlike KC, whose critical loss factor was decreasing with increasing sucrose concentration, the trend of the critical loss factor corresponding to the critical gelling point was not obvious. To further explore the relationship, the fractal dimension (d_f), indicating the density of the structure, was calculated according to Eq. (4) based on critical relaxation exponent *n* and both the results are shown in Fig. 5a. Only the density of 5% sucrose concentration is significantly higher than no sucrose samples. It can also be a reason for the significantly stronger gel as suggested by temperature sweep.

Next, the critical gel strength (S_g) was calculated from Eq. (6). It was reported that an increase in S_g could be related to gel strength (Liu & Li, 2016). According to Fig. 5b, S_g also attained its highest value at 5% sucrose, in agreement with the former results. The normalised S_g was also calculated to eliminate the impact of sucrose concentration (Fig. 5**c**). A sharp decrease in S_g was observed, which differed from the result found for KC. The trend of normalised S_g signifies the contribution of sucrose to the amount and size of junction zones and increasing normalised S_g has been reported to relate to improvements of both junction size and amounts. Therefore, sucrose seems to provide little help since IC has little junction aggregation behaviours as mentioned before.

3.3. Evaluation of the mechanisms underlying the effect of sucrose using the KB theory

The KB theory has been applied to various polymers such as agrose, gelatin, kappa carrageenan, starch and soy proteins (Nicol, Isobe, Clark, Matubayasi, & Shimizu, 2019; Shimizu et al., 2017; Shimizu & Matubayasi, 2014; Stenner et al., 2016), allowing us to calculate ΔG_{u1} and ΔG_{u2}, which represent the potential mechanisms of the stabilisation effect of sucrose on IC gelation. ΔG_{u1} represents the occupation of water structural change, while ΔG_{u2} reveals the contribution of the exclusion effect of water and direct binding between IC and sucrose (Stenner et al., 2016). The calculated results are shown in Table 1. $|\Delta G_{u2}|$ had a significantly larger value than $|\Delta G_{u1}|$ at all concentrations of sucrose and this was similar to the results for KC, which indicated a dominant role of the exclusion effect of water and direct binding between IC and sucrose. IC (G4S-DA2S) has one more sulphated group substitution than KC (G4S-DA) and this might result in fewer reactive sites for IC to bind with sucrose via hydrogen bonds. Thus, for IC, the "saturation" amount of sucrose that could be linked is lower than that of KC. Moreover, the value of $|\Delta G_{u2}|$ is reported to be positively related to the number of equatorial –OH groups. As the concentration of sucrose increased, $|\Delta G_{u2}|$ increased up to 5% and decreased thereafter, which might reveal a reduction in the average number of OH groups at higher concentrations of sucrose.

3.4. Interaction between different amounts of sucrose and IC

FTIR spectroscopy was developed to identify seaweed hydrocolloids by reasonable assignment of the peaks to specific structures. Fig. 6 shows the FTIR spectra of IC with different amount of added sucrose. Pure sucrose was also tested as reference. A broad band at around 3400 cm^{-1} represents O–H stretching of both IC and sucrose. A strong peak appearing at approximately 1639 cm^{-1} indicates the O–C–O bond and glycosidic linkages (Sheng et al., 2018). Characteristic peaks of IC were found in the 0% sample: the strong band at around 845 cm^{-1} is assigned to C–O–SO_4 on C_4 of galactose-4- sulphate (G4S); the signals at around 805 and 905 cm^{-1} are reported to be C–O–SO_4 on C_2 of 3,6-anhydrogalactose (DA2S); and the two peaks at about 935 cm^{-1} and 1070 cm^{-1} suggested C–O bonds of 3,6-anhydrogalactose (DA). The peak at around 1260 cm^{-1} (not found in the sucrose standard) confirmed the presence of the sulphate ester in IC (Pereira, Amado, Critchley, van de Velde, & Ribeiro-Claro, 2009).

In general, IC with different amounts of added sucrose showed

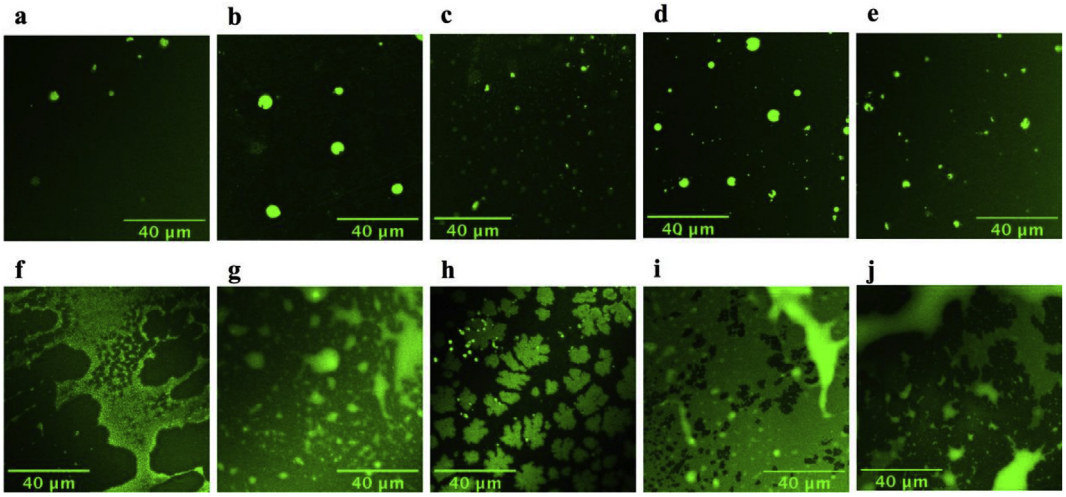

Fig. 9. Microstructure of 0.5% (w/v) solution (a–e) and 2% (w/v) gel (f–j): (a, f) iota carrageenan (IC) with 0% sucrose; (b, g) 2.5% sucrose; (c, h) 5% sucrose; (d, i): 10% sucrose; (e, j) 20% sucrose. *Fluorescein isothiocyanate (FITC, green) was used to stain the IC. (For interpretation of the references to colour in this figure legend, the reader is referred to the Web version of this article.)

similar spectra; however, variations and shifts were observed in specific ranges, which reflected the interaction between IC and sucrose (Moniha, Alagar, Selvasekarapandian, Sundaresan, & Boopathi, 2018). The peak at around 845 cm^{-1} overlaps between IC and sucrose. For IC curves, the peak is only at 845 cm^{-1}. When sucrose in added, there is one more peak at 835 cm^{-1} as shown in Table 2. Similar to KC, this shift is related to the interaction (hydrogen bond formation) between IC and equatorial –OH moieties of sucrose (Yang et al., 2018b). Another variation occurred at C–O–SO_4 on the C_2 of 3,6-anhydrogalactose (DA2S). In the spectrum of IC, peaks appeared at both 805 cm^{-1} and 905 cm^{-1}. However, the addition of sucrose shifted the signal at 905 to 920 cm^{-1}. This also provided evidence of intermolecular hydrogen bond formation.

3.5. Schematic model

A schematic model was produced (Fig. 7) to illustrate the effect on the gelation of IC caused by sucrose addition according to the results of the present study. Similar to KC, IC gelation can be stabilised by sucrose via an exclusion effect of water in solution and by direct binding between sucrose and IC in the gel state (Stenner et al., 2016). Meanwhile, the gelling temperature increases as the sucrose concentration increases (Fig. 1) because of the shift of the equilibrium towards gel formation. However, when it comes to gel strength, unlike KC, there is a "saturation concentration" (5%) for sucrose.

In the range of 0–5% sucrose, hydrogen bonds formed between IC and sucrose seem to be the dominant force to enhance the gel strength. At 5% sucrose, the density reached the critical point (Fig. 3). After 5%, even though the stabilisation effect remains, the gel strength starts to decrease, according to the rheological test (Fig. 1b). The density and cohesive energy presented a similar phenomenon (Table 1 and Fig. 5). The reduction of network density could be caused by heterogeneity in the structure, which is caused by sucrose-sucrose hydrogen bonding. The fewer positions in IC that can form hydrogen bonds could be responsible for the effect. Therefore, excess sucrose tends to form intermolecular hydrogen bonds, according to the KB theory assessment, with a less than average number of equatorial –OH moieties, which are less commonly found than sucrose-water hydrogen bonds. Consequently, the connections between sucrose molecules produce some degree of steric hindrance for IC aggregation and loosens the structure.

3.6. Model validation

3.6.1. Zeta potential

Electrical properties can be used to describe behaviours in solution. The zeta potential reflects the stability of aggregation, higher negative charges, and better stability (Chung, Sher, Rousset, & McClements, 2017). Fig. 8 shows that a small amount of sucrose (< 5%) disturbs the aggregates and produces a denser gel, while higher sucrose concentrations help to stabilise the aggregates in solution. This corresponds with the results from the rheological tests and the Winter-Chambon equation.

3.6.2. CLSM

Microstructures of gels formed with different amounts of added sucrose in 2% IC (solution state of 0.5%, w/v and gel state of 2%, w/v) were studied using CLSM (Fig. 9). FITC was used to stain IC, with no manually adjustment of the image contrast. Therefore, the brightness indicates the concentration of IC. The same scale was used in all samples for a clearer comparison. A homogenous structure with some bright aggregates was observed in all samples: bright dots in solution state (Fig. 9a–e); larger and more connective structure in the gel state (Fig. 9f–j), which agreed with the results of Bui, Nguyen, Renou, and Nicolai (2019). As the addition of sucrose increased, the microstructure also exhibited a similar trend to the previous results. At 5% sucrose addition, a "saturation" state appears in terms of the highest homogeneity in the solution state (Fig. 9c) and the highest uniformity of aggregates in gel state (Fig. 9h). In other words, the density of aggregates increased as the sucrose concentration reached 5%, but decreased at concentrations above 5%. At concentrations of 10% and 20% in the gel state (Fig. 9i and j), IC forms bigger strands, while the distribution of the strands by becomes more uneven.

4. Conclusion

In the present study, the effects of adding sucrose (0–20%) to iota carrageenan on the rheological behaviour and the possible mechanisms were systematically studied. In general, sucrose addition increased the gelling temperature (51.4–57.4 °C), and the relationship between sucrose concentration and gelling temperature could be described using mathematical models. The melting temperature provided a similar trend (52.8–58.8 °C). The exclusion effect of water as well as the bonds between sucrose and carrageenan according to the KB theory probably caused the stabilisation effect. However, the gel strength did not always increase, and 5% sucrose appeared to be the "saturation" concentration to achieve the highest gel strength, as indicated by the zeta potential, rheological test, and CLSM. According to the Winter-Chambon equation, the density of the structure also showed the similar results. Thus, too much sucrose reduced the density of the network. FTIR spectroscopy indicated the binding between sucrose and carrageenan through hydrogen bonds. At higher concentrations (> 5%), sucrose–sucrose hydrogen bonds might form to produce a kind of steric hindrance that would loosen the network of carrageenan, because the KB theory indicated a less than average equatorial –OH. A scheme was proposed to describe the effects of sucrose addition at different concentrations that showed the possible bonds responsible for the observed effects.

Conflicts of interest

We declare that we have no commercial or associative interest that represents a conflict of interest in connection with this manuscript. We have no financial and personal relationships with other people or organisations that can inappropriately influence our work.

Acknowledgements

This work was funded by the Singapore NRF Industry-IHL Partnership Grant (R-143-000-653-281) and student support (R-143-002-653-281).

Appendix A. Supplementary data

Supplementary data to this article can be found online at https://doi.org/10.1016/j.foodhyd.2019.105317.

References

Agoda-Tandjawa, G., Le Garnec, C., Boulenguer, P., Gilles, M., & Langendorff, V. (2017). Rheological behavior of starch/carrageenan/milk proteins mixed systems: Role of each biopolymer type and chemical characteristics. *Food Hydrocolloids, 73*, 300–312.

Ali, A. M. M., Kishimura, H., & Benjakul, S. (2018). Physicochemical and molecular properties of gelatin from skin of golden carp (*Probarbus Jullieni*) as influenced by acid pretreatment and prior-ultrasonication. *Food Hydrocolloids, 82*, 164–172.

Bixler, H. J., & Porse, H. (2011). A decade of change in the seaweed hydrocolloids industry. *Journal of Applied Phycology, 23*(3), 321–335.

Brenner, T., Tuvikene, R., Parker, A., Matsukawa, S., & Nishinari, K. (2014). Rheology and structure of mixed kappa-carrageenan/iota-carrageenan gels. *Food Hydrocolloids, 39*, 272–279.

Bui, V. T. N. T., Nguyen, B. T., Renou, F., & Nicolai, T. (2019). Rheology and microstructure of mixtures of iota and kappa-carrageenan. *Food Hydrocolloids, 89*, 180–187.

Chung, C., Sher, A., Rousset, P., & McClements, D. J. (2017). Use of natural emulsifiers in model coffee creamers: Physical properties of quillaja saponin-stabilized emulsions. *Food Hydrocolloids, 67*, 111–119.

Covis, R., Guegan, J.-P., Jeftić, J., Czjzek, M., Benoit, M., & Benvegnu, T. (2016). Structural and rheological properties of kappa (κ)-carrageenans covalently modified

with cationic moieties. *Journal of Polymer Research, 23*(4), 78.
Diañez, I., Gallegos, C., Brito-de la Fuente, E., Martínez, I., Valencia, C., Sánchez, M. C., et al. (2019). 3D printing in situ gelification of κ-carrageenan solutions: Effect of printing variables on the rheological response. *Food Hydrocolloids, 87*, 321–330.
Dong, Y., Wen, C., Li, T., Wu, C., Qi, H., Liu, M., et al. (2019). The effects of amino acids on the gel properties of potassium iota carrageenan. *Food Hydrocolloids, 95*, 378–384.
Gabriele, D., de Cindio, B., & D'Antona, P. (2001). A weak gel model for foods. *Rheologica Acta, 40*(2), 120–127.
Gekko, K., & Kasuya, K. (1985). Effect of pressure on the sol-gel transition of carrageenans. *International Journal of Biological Macromolecules, 7*(5), 299–306.
Gekko, K., Mugishima, H., & Koga, S. (1987). Effects of sugars and polyols on the sol-gel transition of κ-carrageenan: Calorimetric study. *International Journal of Biological Macromolecules, 9*(3), 146–152.
Huang, M., & Yang, H. (2019). Eucheuma powder as a partial flour replacement and its effect on the properties of sponge cake. *LWT-Food Science and Technology, 110*, 262–268.
Kirkwood, J. G., & Buff, F. P. (1951). The statistical mechanical theory of solutions. I. *The Journal of Chemical Physics, 19*(6), 774–777.
Lethuaut, L., Brossard, C., Rousseau, F., Bousseau, B.t., & Genot, C. (2003). Sweetness–texture interactions in model dairy desserts: Effect of sucrose concentration and the carrageenan type. *International Dairy Journal, 13*(8), 631–641.
Liu, S., & Li, L. (2016). Thermoreversible gelation and scaling behavior of Ca2+- induced κ-carrageenan hydrogels. *Food Hydrocolloids, 61*, 793–800.
Li, T., Wen, C., Dong, Y., Li, D., Liu, M., Wang, Z., et al. (2019). Effect of ε-polylysine addition on κ-carrageenan gel properties: Rheology, water mobility, thermal stability and microstructure. *Food Hydrocolloids, 95*, 212–218.
Moniha, V., Alagar, M., Selvasekarapandian, S., Sundaresan, B., & Boopathi, G. (2018). Conductive bio-polymer electrolyte iota-carrageenan with ammonium nitrate for application in electrochemical devices. *Journal of Non-crystalline Solids, 481*, 424–434.
Motta Romero, H., Santra, D., Rose, D., & Zhang, Y. (2017). Dough rheological properties and texture of gluten-free pasta based on proso millet flour. *Journal of Cereal Science, 74*, 238–243.
Nguyen, B. T., Nicolai, T., Benyahia, L., & Chassenieux, C. (2014). Synergistic effects of mixed salt on the gelation of κ-carrageenan. *Carbohydrate Polymers, 112*, 10–15.
Nicol, T. W. J., Isobe, N., Clark, J. H., Matubayasi, N., & Shimizu, S. (2019). The mechanism of salt effects on starch gelatinization from a statistical thermodynamic perspective. *Food Hydrocolloids, 87*, 593–601.
Pang, Z., Xu, R., Luo, T., Che, X., Bansal, N., & Liu, X. (2019). Physiochemical properties of modified starch under yogurt manufacturing conditions and its relation to the properties of yogurt. *Journal of Food Engineering, 245*, 11–17.
Parker, A., Brigand, G., Miniou, C., Trespoey, A., & Vallée, P. (1993). Rheology and fracture of mixed ι- and κ-carrageenan gels: Two-step gelation. *Carbohydrate Polymers, 20*(4), 253–262.
Pereira, L., Amado, A. M., Critchley, A. T., van de Velde, F., & Ribeiro-Claro, P. J. A. (2009). Identification of selected seaweed polysaccharides (phycocolloids) by vibrational spectroscopy (FTIR-ATR and FT-Raman). *Food Hydrocolloids, 23*(7), 1903–1909.
Piculell, L. (2006). *Gelling carrageenans.* Boca Raton: CRC Press.
Piculell, L., Nilsson, S., & Muhrbeck, P. (1992). Effects of small amounts of kappa- carrageenan on the rheology of aqueous iota-carrageenan. *Carbohydrate Polymers, 18*(3), 199–208.
Piorkowski, D. T., & McClements, D. J. (2014). Beverage emulsions: Recent developments in formulation, production, and applications. *Food Hydrocolloids, 42*, 5–41.
Rafe, A., & Razavi, S. M. A. (2017). Scaling law, fractal analysis and rheological characteristics of physical gels cross-linked with sodium trimetaphosphate. *Food Hydrocolloids, 62*, 58–65.
Sharma Khanal, B. K., Budiman, C., Hodson, M. P., Plan, M. R. R., Prakash, S., Bhandari, B., et al. (2019). Physico-chemical and biochemical properties of low fat Cheddar cheese made from micron to nano sized milk fat emulsions. *Journal of Food Engineering, 242*, 94–105.
Sheng, L., Li, P., Wu, H., Liu, Y., Han, K., Gouda, M., et al. (2018). Tapioca starch-pullulan interaction during gelation and retrogradation. *LWT-Food Science and Technology, 96*, 432–438.
Shimizu, S., & Boon, C. L. (2004). The Kirkwood–Buff theory and the effect of cosolvents on biochemical reactions. *The Journal of Chemical Physics, 121*(18), 9147–9155.
Shimizu, S., & Matubayasi, N. (2014). Gelation: The role of sugars and polyols on gelatin and agarose. *The Journal of Physical Chemistry B, 118*(46), 13210–13216.
Shimizu, S., Stenner, R., & Matubayasi, N. (2017). Gastrophysics: Statistical thermodynamics of biomolecular denaturation and gelation from the Kirkwood-Buff theory towards the understanding of tofu. *Food Hydrocolloids, 62*, 128–139.
Soukoulis, C., Fisk, I. D., Gan, H.-H., & Hoffmann, L. (2016). Intragastric structuring of anionic polysaccharide kappa-carrageenan filled gels under physiological in vitro digestion conditions. *Journal of Food Engineering, 191*, 105–114.
Sow, L. C., Chong, J. M. N., Liao, Q. X., & Yang, H. (2018a). Effects of κ-carrageenan on the structure and rheological properties of fish gelatin. *Journal of Food Engineering, 239*, 92–103.
Sow, L. C., Kong, K., & Yang, H. (2018b). Structural modification of fish gelatin by the addition of gellan, κ-carrageenan, and salts mimics the critical physicochemical properties of pork gelatin. *Journal of Food Science, 83*(5), 1280–1291.
Sow, L. C., Tan, S. J., & Yang, H. (2019a). Rheological properties and structure modification in liquid and gel of tilapia skin gelatin by the addition of low acyl gellan. *Food Hydrocolloids, 90*, 9–18.
Sow, L. C., Toh, N. Z. Y., Wong, C. W., & Yang, H. (2019b). Combination of sodium alginate with tilapia fish gelatin for improved texture properties and nanostructure modification. *Food Hydrocolloids, 94*, 459–467.
Stenner, R., Matubayasi, N., & Shimizu, S. (2016). Gelation of carrageenan: Effects of sugars and polyols. *Food Hydrocolloids, 54*, 284–292.
Watase, M., Nishinari, K., Williams, P. A., & Phillips, G. O. (1990). Agarose gels: Effect of sucrose, glucose, urea, and guanidine hydrochloride on the rheological and thermal properties. *Journal of Agricultural and Food Chemistry, 38*(5), 1181–1187.
Wu, Y., Guo, R., Cao, N., Sun, X., Sui, Z., & Guo, Q. (2018). A systematical rheological study of polysaccharide from *Sophora alopecuroides* L. seeds. *Carbohydrate Polymers, 180*, 63–71.
Yang, K., Wang, Z., Brenner, T., Kikuzaki, H., Fang, Y., & Nishinari, K. (2015). Sucrose release from agar gels: Correlation with sucrose content and rheology. *Food Hydrocolloids, 43*, 132–136.
Yang, Z., Yang, H., & Yang, H. (2018a). Characterisation of rheology and microstructures of κ-carrageenan in ethanol-water mixtures. *Food Research International, 107*, 738–746.
Yang, Z., Yang, H., & Yang, H. (2018b). Effects of sucrose addition on the rheology and microstructure of κ-carrageenan gel. *Food Hydrocolloids, 75*, 164–173.
Zhong, Q., & Ikeda, S. (2012). Viscoelastic properties of concentrated aqueous ethanol suspensions of α-zein. *Food Hydrocolloids, 28*(1), 46–52.
Zhou, Y., & Yang, H. (2019). Effects of calcium ion on gel properties and gelation of tilapia (*Oreochromis niloticus*) protein isolates processed with pH shift method. *Food Chemistry, 277*, 327–335.
Zia, K. M., Tabasum, S., Nasif, M., Sultan, N., Aslam, N., Noreen, A., et al. (2017). A review on synthesis, properties and applications of natural polymer based carrageenan blends and composites. *International Journal of Biological Macromolecules, 96*, 282–301.